Unity and Discord in Opinion Dynamics

E. Ben-Naim[†], P. L. Krapivsky[‡], F. Vazquez[†], and S. Redner[‡]

[†]*Theoretical Division and Center for Nonlinear Studies, Los Alamos National Laboratory, Los Alamos, New Mexico, 87545*

[‡]*Center for BioDynamics, Center for Polymer Studies, and Department of Physics, Boston University, Boston, MA, 02215*

Abstract

We study opinion dynamics models where agents evolve via repeated pairwise interactions. In the compromise model, agents with sufficiently close real-valued opinions average their opinions. A steady state is reached with a finite number of isolated, noninteracting opinion clusters ("parties"). As the initial opinion range increases, the number of such parties undergoes a periodic bifurcation sequence, with alternating major and minor parties. In the constrained voter model, there are leftists, centrists, and rightists. A centrist and an extremist can both become centrists or extremists in an interaction, while leftists and rightists do not affect each other. The final state is either consensus or a frozen population of leftists and rightists. The evolution in one dimension is mapped onto a constrained spin-1 Ising chain with zero-temperature Glauber kinetics. The approach to the final state exhibits a non-universal long-time tail.

Key words: opinion dynamics, bifurcations, voter model, Glauber kinetics
PACS: 02.50.Cw, 05.45.-a, 64.60.My, 75.40.Gb, 89.65.-s,

---

1 Introduction

Opinions of individuals in a heterogeneous society evolve due to influences of acquaintances. In principle, opinions could evolve forever, consensus could emerge, or a population could condense into a finite set of distinct opinion clusters, or "parties". The modeling of such phenomena, both by social scientists [1–3] and by statistical physicists [4–8] is a vibrant area. In this contribution to the Randomness and Complexity conference in honor of Shlomo Havlin's 60th birthday, we discuss two simple models for this type of opinion evolution.

In the *compromise model* [9,10], the opinion of each individual is a real-valued variable on a finite range. In an interaction, two compatible agents average

their current opinions, while there is no interaction between agents whose opinion difference exceeds a specified threshold. These rules model the competition between compromise and conviction as a function of the opinion difference of two individuals. To implement the dynamics, two agents are picked at random and they interact if compatible. This basic step is repeated *ad infinitum.*

A simplified stochastic version of this process is the *constrained voter model* [11]. Here, each individual has three states — leftist, centrist, and rightist. In an event, an agent adopts the opinion of a randomly-chosen neighbor, as in the voter model [12], but with the proviso that leftists and rightists do not interact. Due to this constraint, the outcome can be either consensus or a frozen mixture of extremists with no centrists.

2   Compromise Model

In an interaction, agents with opinions x_1 and x_2 (with $|x_2 - x_1| < 1$) average their opinions: $(x_1, x_2) \rightarrow \frac{1}{2}(x_1 + x_2, x_1 + x_2)$; if $|x_2 - x_1| > 1$, no interaction occurs. Let $P(x,t)\,dx$ be the fraction of agents with opinions in the range $[x, x + dx]$ at time t. This distribution evolves according to [10]

$$\frac{\partial}{\partial t}P(x,t) = \iint dx_1 dx_2 P(x_1,t)P(x_2,t)\left[\delta\left(x - \frac{x_1 + x_2}{2}\right) - \delta(x - x_1)\right], \quad (1)$$

where the integration is over all $|x_1 - x_2| < 1$. When all agents can interact, namely, when $\Delta < 1/2$, the rate equations are integrable [13,14]. In particular, the second moment vanishes as $M_2(t) = M_2(0)\,e^{-M_0 t/2}$, with $M_0 = 2\Delta$, where $M_k(t) \equiv \int dx\, x^k\, P(x,t)$ is the kth moment. The distribution itself approaches consensus as $P(x,t) \propto M_0/[w(1 + z^2)^2]$ [14], with variance $w = M_2^{1/2}/M_0$ and scaling variable $z = x/w$.

For larger values of Δ, the opinion distribution does not condense into a single cluster, but rather the distribution evolves into "parties" that are separated by distances larger than one. This behavior results from an instability that propagates from the boundary toward the center (Fig. 1). Once each party is isolated, it then separately evolves into a delta function so that the final distribution consists of a series of non-interacting delta-function clusters.

Numerical integration of the rate equations reveals [10] a striking bifurcation sequence in the cluster (party) locations (Fig. 1). There are three types of clusters: major (mass $M > 1$), minor (mass $m < 10^{-2}$), and a central cluster located exactly at $x = 0$. When $\Delta < 1$, the final state is a single peak located at the origin. When $\Delta > 1$, two new clusters are born at the extreme edges, $x \approx \pm\Delta$. As Δ increases, three basic bifurcations occur:

(1) Nucleation of a symmetric cluster pair: $\emptyset \to \{-x, x\}$ with $x \approx 1$.
(2) Annihilation of the central cluster and simultaneous nucleation of a symmetric cluster pair: $\{0\} \to \{-x, x\}$ with $x \approx 0.75$.
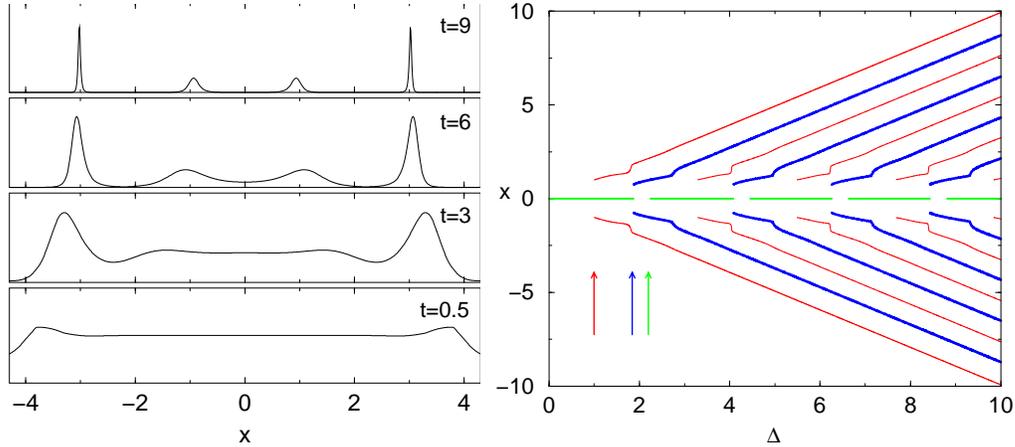(3) Nucleation of a central cluster: $\emptyset \to \{0\}$.

Fig. 1. (Left) Early-time evolution of the opinion distribution $P(x, t)$ for $\Delta = 4.3$. (Right) Location of final state clusters versus initial opinion range Δ (red: clusters via type-1 bifurcations, blue: type-2, green: type-3). The color coded vertical arrows indicate the location of the first 3 bifurcations.

The cluster masses vary periodically in Δ and organize in an alternating major-minor pattern. The major clusters contain nearly the entire system mass, while the minor clusters are much smaller (Fig. 2). Near a type-3 bifurcation, a central cluster nucleates with infinitesimal mass, initially grows slowly, then explosively until its mass becomes of order one. Finally, its mass grows linearly with Δ. At the next type-2 bifurcation threshold, the central cluster then splits into two major clusters (Fig. 2). This birth-and-death pattern repeats.

The minor clusters exhibit two subtle features. First, the mass of the most extreme cluster saturates to a mass m' that is approximately one order of magnitude greater than all other minor clusters. Second, the mass of the minor clusters varies non-monotonically with Δ, and there is a small range of Δ, where the mass of a newly-born minor cluster suddenly drops (Fig. 2) before the mass saturates.

At type-1 and type-3 bifurcations, the mass of the nascent clusters varies as $m \sim (\Delta - \Delta_n)^{\alpha_n}$ as $\Delta \to \Delta_n$. The exponent depends only on the type n of the bifurcation point; numerically we find $\alpha_1 \approx 3$ and $\alpha_3 \approx 4$. To understand the behavior near a type-1 bifurcation, consider the first one at $\Delta_1 = 1$. Let $\Delta = 1 + \epsilon$ with $\epsilon \to 0$. It is convenient to divide the opinion range $(-\Delta, \Delta)$ into a central subinterval $(-1, 1)$ and two boundary subintervals: $\pm(1, 1 + \epsilon)$. Let $m(t)$ be the mass in a boundary subinterval. This mass decays due to the interaction with agents in the central subinterval. As a result, $\dot{m} = -m$, which together with the initial condition $m(0) = \epsilon$, gives $m(t) = \epsilon\, e^{-t}$.
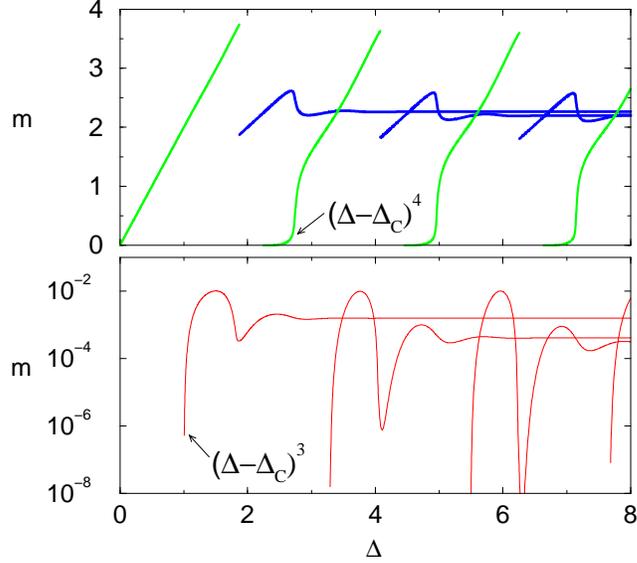
Fig. 2. Cluster mass versus opinion range (same color scheme as Fig. 1). The central clusters (green) and the major clusters (blue) are shown on a linear scale (top), while the minor clusters (red) are shown on a logarithmic scale (bottom).

On the other hand, the mass of the central subinterval is concentrated in a region about the origin whose width $w(t)$ decreases with time. At some moment t_f the separation between the masses in the central and boundary subintervals exceeds unity. If we assume that the mass in the boundary subinterval is at its center, $x = 1 + \epsilon/2$, the separation criterion is $w(t_f) \sim \epsilon/2$. For $t \gg t_f$, the interaction between the two subintervals stops and the mass of the emerging minor cluster freezes at $m_f \sim \epsilon\, e^{-t_f}$.

We estimate the width $w(t)$ by noting that, to zeroth order in ϵ, (i) the central subinterval is not affected by boundary subintervals, and (ii) all agents are eventually within the interaction range. Therefore the asymptotic time dependence of $w(t)$ is the same as in the case $\Delta < 1/2$. Thus $w(t) \sim M_2^{1/2} \sim e^{-t/2}$, since $\Delta = 1 + \epsilon \cong 1$. Using the stopping criterion, $w(t_f) \sim e^{-t_f/2} \sim \epsilon$, the final minor cluster mass is $m_f \sim \epsilon\, e^{-t_f} \sim \epsilon^3$, leading to $\alpha_1 = 3$. For a type-3 bifurcation, a similar argument yields $\alpha_3 = 4$ [10].

3   Constrained Voter Model

The constrained voter model is a simple discrete-state version of the previous compromise model in which each agent can have one of the three opinions of leftist, centrist, and rightist. Similar to the compromise model, agents with nearby opinions can interact, while agents with distant opinions cannot. Thus in an interaction, a centrist and an extremist (either on the left or the right)

4

can both become centrists or both become extremists of the same persuasion as the initial extremist. Notice that this interaction is not compromise, but rather one agent convinces the other, as in the classic voter model. The three-state model is the simplest discrete system that embodies the constraint of the compromise model.

The constrained voter model is also equivalent to a constrained spin-1 Ising system with $T = 0$ Glauber kinetics [15]. Leftist, centrist, and rightist opinions are equivalent to the respective spin states $-$, 0, and $+$. By the incompatibility of leftists and rightists, neighboring $+$ and $-$ spins do not interact. Thus an arbitrary initial state could evolve to a static final state that contains only $+$ and $-$ spins (Fig. 3).

If we temporarily disregard the difference between leftists and rightists, the resulting binary system of centrists and extremists reduces to the voter model, for which one of two absorbing states — either all centrists or all extremists — is eventually reached. In the context of the three-opinion system, the latter is either consensus of extremists or a frozen state of leftists and rightists.
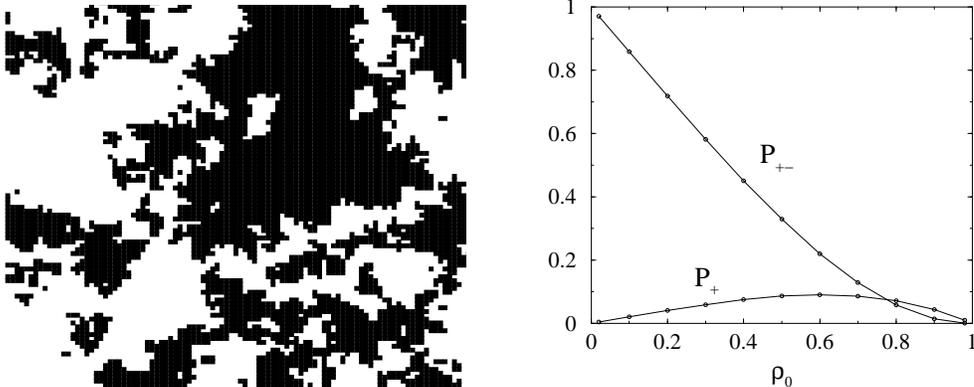

Fig. 3. (Left) Typical frozen final state of $+$ and $-$ on a 100×100 square for $\rho_0 = 0.1$. Notice the nested enclaves of opposite opinions. (Right) Probability for the occurrence of a given final state as a function of ρ_0 for $\rho_+ = \rho_-$.

Because of the underlying voter dynamics, the average density of each species is globally conserved in any spatial dimension [12]. Thus $\langle \rho_i(t) \rangle = \rho_i(t = 0)$, where i refers to one of the states $(+, 0, -)$ and the angle brackets denote an average over all dynamical trajectories and all initial states with the specified densities. By the conservation of the magnetization, the final state consists of all centrists with probability $P_0 = \rho_0$, where ρ_0 is the initial density of 0-spins, and with probability $1 - \rho_0$ there are no centrists in the final state. In the latter case, there can be either a consensus of $+$ (with probability $P_+(\rho_0)$), consensus of $-$ (probability $P_-(\rho_0)$), or a frozen mixed state (probability $P_{+-}(\rho_0)$). Figure 3 shows the dependence of these final state probabilities on ρ_0 in the mean-field limit in the symmetric case $\rho_+ = \rho_- = (1 - \rho_0)/2$; nearly identical results occur in one and two dimensions.

A good way to visualize the dynamics in one dimension is in terms of domain walls (Fig. 4). There are three types of walls: diffusing walls between $+0$ and between -0, respectively denoted by M_+ and M_-, and stationary domain walls S between $+-$. The mobile walls evolve by

$$M_\pm + M_\pm \to \emptyset, \qquad M_\pm + M_\mp \to S. \tag{2}$$

When a mobile wall hits a stationary wall, the former changes its sign while the latter is eliminated via the reaction

$$M_\pm + S \to M_\mp. \tag{3}$$

Any initial opinion state forces two important topological constraints in the domain wall arrangement: (i) an *even* number of mobile walls between each pair of stationary wall, and (ii) prohibition of domain wall sequences of the form $\dots M_+ M_- M_+ \dots$. These constraints play a crucial role in the kinetics; related kinetic constraints arise in models of glassy dynamics [16].
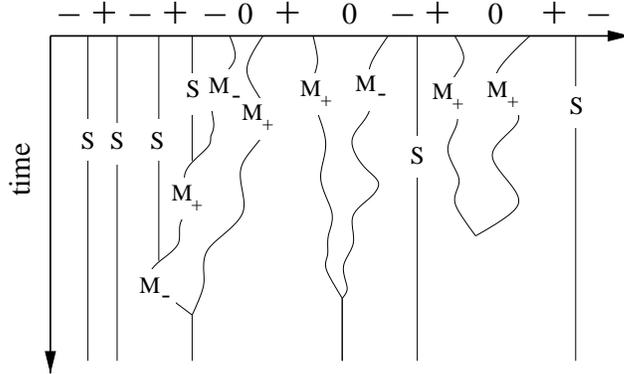

Fig. 4. Space-time representation of the domain wall dynamics. Time runs vertically downward. The spin state of the domains and the identity of each domain wall are indicated.

Simulations show that the stationary domain wall density decays extremely slowly: $S(t) \sim t^{-\psi}$ with $\psi(\rho_0) \to 0$ as $\rho_0 \to 0$ [11]. To understand this slow decay, consider the rate equation for the stationary domain wall density

$$\dot{S} = -k\, M\, S. \tag{4}$$

While such a rate equation is generally inapplicable in low spatial dimension, we can adapt it to one dimension by employing an effective time-dependent reaction rate: $k \simeq \sqrt{2/\pi t}$ [11,17]. This is the time-dependent flux to an absorbing point due to a uniform initial density of diffusing particles; such a rate phenomenologically accounts for spatial fluctuations in one dimension.

As $\rho_0 \to 0$, the system initially consists of long strings of stationary walls that are interspersed by pairs of more closely-spaced mobile walls. Their survival probability is proportional to their initial separation, so that the asymptotic density of mobile walls is $M \simeq 2\rho_0/\sqrt{\pi t}$ [11]. Substituting this expression for $M(t)$ and the above reaction rate into this rate equation, the density of stationary walls decays as $t^{-\psi}$ with $\psi(\rho_0) = \sqrt{8}\,\rho_0/\pi$ as $\rho_0 \to 0$. A more compelling approach in terms of the persistence in the q-state Potts model [18,19] gives $\psi(\rho_0) \to 2\rho_0/\pi$ as $\rho_0 \to 0$, in excellent agreement with our numerics [10].

4   Outlook and Application

Minimalist opinion dynamics models exhibit a variety of intriguing properties. The competition between interaction among compatible individuals and rigidity among incompatible individuals leads to rich dynamics and to complex final states. The preliminary results reported here suggest many avenues for future theoretical research. For example, in the compromise model, what types of bifurcation patterns emerge with different initial conditions? What happens when the opinion space is multidimensional? What is the overall approach rate to the final state?

We offer the Canadian federal elections of 1993 as a realization of the compromise model [20]. For most of its history Canada had two major political parties: Liberal (L) and Conservative, the latter morphing into the Progressive Conservative (PC) party after 1930. After 1945 a third national party appeared, the leftist New Democratic Party (NDP). This near stasis was dramatically altered in the 1993 election when the polity broke up into 5 primarily regional parties. This fragmentation reflected the timely tensions of separatism in Quebec and federalist disaffection in the west, a feature that is roughly equivalent to an increase in the opinion range Δ. In the election, the newly-created right-wing Reform party captured 52/295 parliamentary seats, with all but 2 in the 3 westernmost provinces. The Bloc Quebecois captured 54 seats exclusively in Quebec. The liberals won the election handily, garnering a majority of 177 seats, but they were a miniscule presence in the west. The NDP captured 9 seats, but only in the west. The PC party won only 2 seats! This political fragmentation could well represent a bifurcation in the compromise model.

In the constrained voter model, even simpler theoretical questions are still not well understood. Most notably, what is the probability of reaching a given final state as a function of the initial condition? More quantitatively, what are the dependences of $P_+(\rho_0)$ and $P_{+-}(\rho_0)$ on the initial density of 0-spins ρ_0?

At a practical level, the constrained voter model may be useful for under-

standing the political evolution in countries where people of centrist persua-
sion gradually get converted to more extreme positions. This can result in the
society becoming more polarized, with relatively ineffectual political discourse
between the remaining parties. Possible examples of a such situation possibly
include Northern Ireland (unionists vs. nationalists) and Israel (secularists vs.
religious parties).

5 Acknowledgements

References

[1] H. Föllmer, J. Math. Econ. **1**, 51 (1974); J. Kobayashi, J. Math. Sociology **24**, 285 (2001); R. Hegselmann and U. Krause, J. Artif. Soc. Soc. Simul. **5**, no. 3 (2002); ¡http://jasss.soc.surrey.ac.uk/5/3/2.html¿, and references therein.

[2] R. Axelrod, J. Conflict Resolution **41**, 203 (1997); R. Axelrod, *The Complexity of Cooperation*, (Princeton University Press, 1997).

[3] W. Weidlich, *Sociodynamics: A Systematic Approach to Mathematical Modelling in the Social Sciences* (Harwood Academic Publishers, 2000).

[4] S. Galam, Y. Gefen, and Y. Shapir, Math. J. of Sociology **9**, 1 (1982); S. Galam and S. Moscovici, Eur. J. Soc. Psych. **21**, 49 (1991); S. Galam, Physica A **274**, 132 (1999); *cond-mat*/0211571.

[5] C. Castellano, M. Marsili, and A. Vespignani, Phys. Rev. Lett. **85**, 3536 (2000); D. Vilone, A. Vespignani, and C. Castellano, *cond-mat*/0210413.

[6] K. Sznajd-Weron and J. Sznajd, Int. J. Mod. Phys. C **11**, 1157 (2000).

[7] J. Holyst, K. Kacperski, and F. Schweitzer, in: *Annual Reviews of Computational Physics IX*, ed. D. Stauffer (World Scientific, Singapore 2001), pp. 253-273.

[8] D. Stauffer, J. Artif. Soc. Soc. Simul. **5**, no. 1 (2002); ¡http://www.soc.surrey.ac.uk/JASSS/5/1/4.html¿.

[9] G. Weisbuch, G. Deffuant, F. Amblard, and J. P. Nadal, *cond-mat*/0111494; D. Neau, Ph.D. thesis, unpublished.

[10] E. Ben-Naim, P. L. Krapivsky, and S. Redner, Physica D **183**, 190 (2003); also cond-mat/0212313.

[11] F. Vazquez, P. L. Krapivsky, and S. Redner, J. Phys. A **36**, L61 (2003).

[12] T. M. Liggett, *Interacting Particle Systems* (Springer-Verlag, New York, 1985).

[13] E. Ben-Naim and P. L. Krapivsky, Phys. Rev. E **61**, R5 (2000).

[14] A. Baldassarri, U. M. B. Marconi, and A. Puglisi, Europhys. Lett. **58**, 14 (2001).

[15] R. J. Glauber, J. Math. Phys. **4**, 294 (1963).

[16] For a recent review, see F. Ritort and P. Sollich, Adv. Phys. **52**, 219 (2003); also cond-mat/0210382.

[17] S. Redner, *A Guide to First-Passage Processes*, (Cambridge University Press, New York, 2001).

[18] C. Sire and S. N. Majumdar, Phys. Rev. E **52**, 244 (1995).

[19] B. Derrida, V. Hakim, and V. Pasquier, Phys. Rev. Lett. **75**, 751 (1995).

[20] Election results for Canadian elections were obtained from http://www.elections.ca/ and http://polisci.nelson.com/elections.html.